Supplementary Information (SI) for Catalysis Science & Technology.

Supporting information to

Tangled effects of CuCl precursor and Zn, Sn promoters used for the methylchlorosilanes direct synthesis

L. Riviere[1], E. Blaser[2], C. Rosier[2], M. Huet[2], C. Geantet[1] and S. Loridant[1,*]

[1] Université Claude Bernard Lyon 1, CNRS, IRCELYON, UMR 5256, Villeurbanne, F-69100, France

[2] R&D Laboratory, Elkem Silicones France, 69190 Saint Fons, France

*stephane.loridant@ircelyon.univ-lyon1.fr

Thermodynamic calculations

Standard enthalpy of formation at 583 K:

$$\Delta_f H(583\ K) = \Delta_f H(298\ K) + Cp \times (583 - 298)$$

with $\Delta_f H(298\ K)$ the standard enthalpy of formation at 298 K, C_p the heat capacity.

Standard entropy of formation at 583 K:

$$\Delta S°(583\ K) = \Delta S°(298\ K) + Cp \times Ln(\frac{583}{298})$$

with $\Delta S°(298\ K)$ the standard entropy of formation at 298 K.

Table S1. Heat capacities, standard enthalpies and standard entropies of formation of different compounds.

Compound	**C_p (600 K) ($kJ.mol^{-1}.K^{-1}$)**	**Ref.**	**$\Delta_f H$ (583 K) ($kJ.mol^{-1}$)**	**$\Delta_f H$ (298 K) ($kJ.mol^{-1}$)**	**Ref.**	**ΔS° (583 K) ($kJ.mol^{-1}.K^{-1}$)**	**ΔS° (298 K) ($kJ.mol^{-1}.K^{-1}$)**	**Ref.**
Si (s)	0.0200	S1	0	0	S1	0.032	0.019	S1
Cu (s)	0.0244	S1	0	0	S1	0.050	0.033	S1
CuCl (s)	0.0485	S1	-123.4	-137.2	S1	0.118	0.086	S1
$SiCl_4$ (g)	0.1020	S2	-632.9	-662.2	S2	0.399	0.331	S2
Cu_3Si (s)[a]	0.0233	S3	-7.0	-13.6	S4	0.023	0.007	S5
$Cu_{3.75}Si$ (s)[a,b]	0.0235	S3	-4.4	-11.1	S6	0.022	0.007	S5
Cu_5Si (s)[a]	0.0237	S3	-3.8	-10.5	S4	0.021	0.006	S5

[a]: the calculation of heat capacities of copper-silicon silicide was performed by using the Neumann-Kopp rule: $Cp(Cu_xSi_y) = \frac{x \times Cp(Cu) + y \times Cp(Si)}{x + y}$

[b]: $Cu_{3.75}Si$ corresponds to $Cu_{15}Si_4$.

Standard enthalpy of reaction:

$$\Delta_r H°(583\ K) = \sum(v_p \times \Delta_f H°(583\ K)_p) - \sum(v_r \times \Delta_f H°(583\ K)_r)$$

with v_p and v_r the stoichiometric coefficients of products and reactants, respectively.

Standard entropy of reaction:

$$\Delta_r S°(583\ K) = \sum(v_p \times S°(583\ K)_p) - \sum(v_r \times S°(583\ K)_r)$$

Gibbs free energy:

$$\Delta_r G°(583\ K) = \Delta_r H°(583\ K) - 583 \times \Delta S°(583\ K)$$

Table S2. Standard enthalpies and entropies of reaction and Gibbs free energies of different compounds.

Reaction	$\Delta_r H°(583\ K)$ **(kJ.mol^{-1})**	$\Delta_r S°(583\ K)$ **(kJ.mol^{-1}.K^{-1})**	$\Delta_r G°(583\ K)$ **(kJ.mol^{-1})**
$4\ CuCl_{(s)} + Si_{(s)} \rightarrow 4\ Cu_{(s)} + SiCl_{4(g)}$	-139.4	0.089	-191.6
$20\ CuCl_{(s)} + 9\ Si_{(s)} \rightarrow 4\ Cu_5Si_{(s)} + 5\ SiCl_{4(g)}$	-711.8	-0.584	-370.8
$15\ CuCl_{(s)} + 7.75\ Si_{(s)} \rightarrow 4\ Cu_{3.75}Si_{(s)} + 3.75\ SiCl_{4(g)}$	-540.3	-0.446	-280.4
$12\ CuCl_{(s)} + 7\ Si_{(s)} \rightarrow 4\ Cu_3Si_{(s)} + 3\ SiCl_{4(g)}$	-445.9	-0.362	-234.9

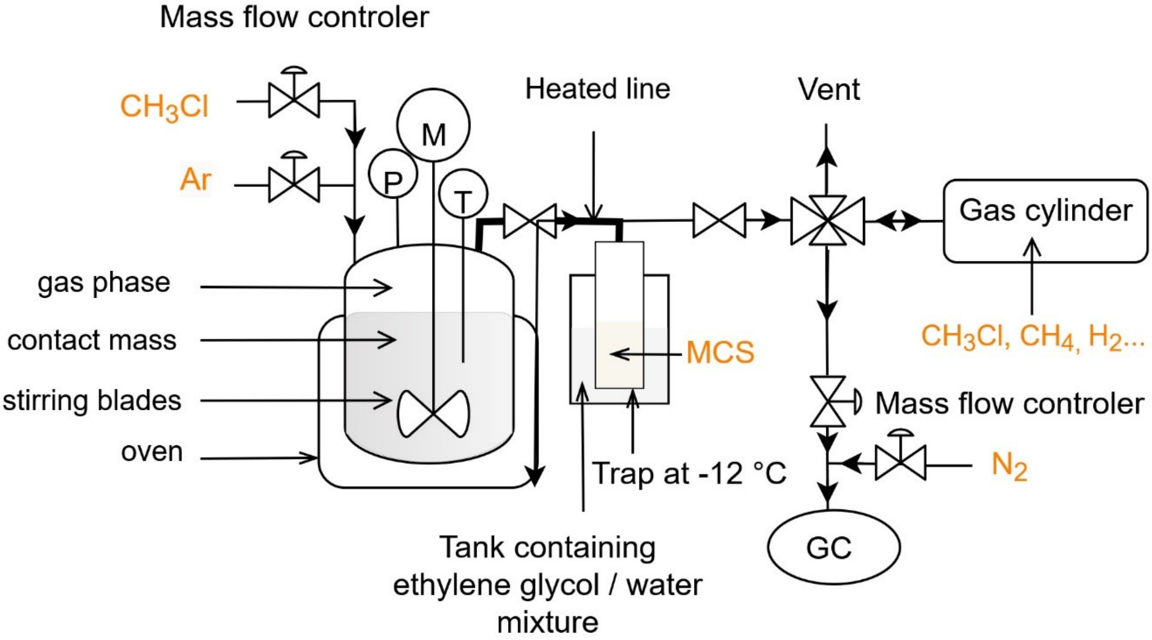

Figure S1. Experimental apparatus for catalytic testing in stirred batch reactor.

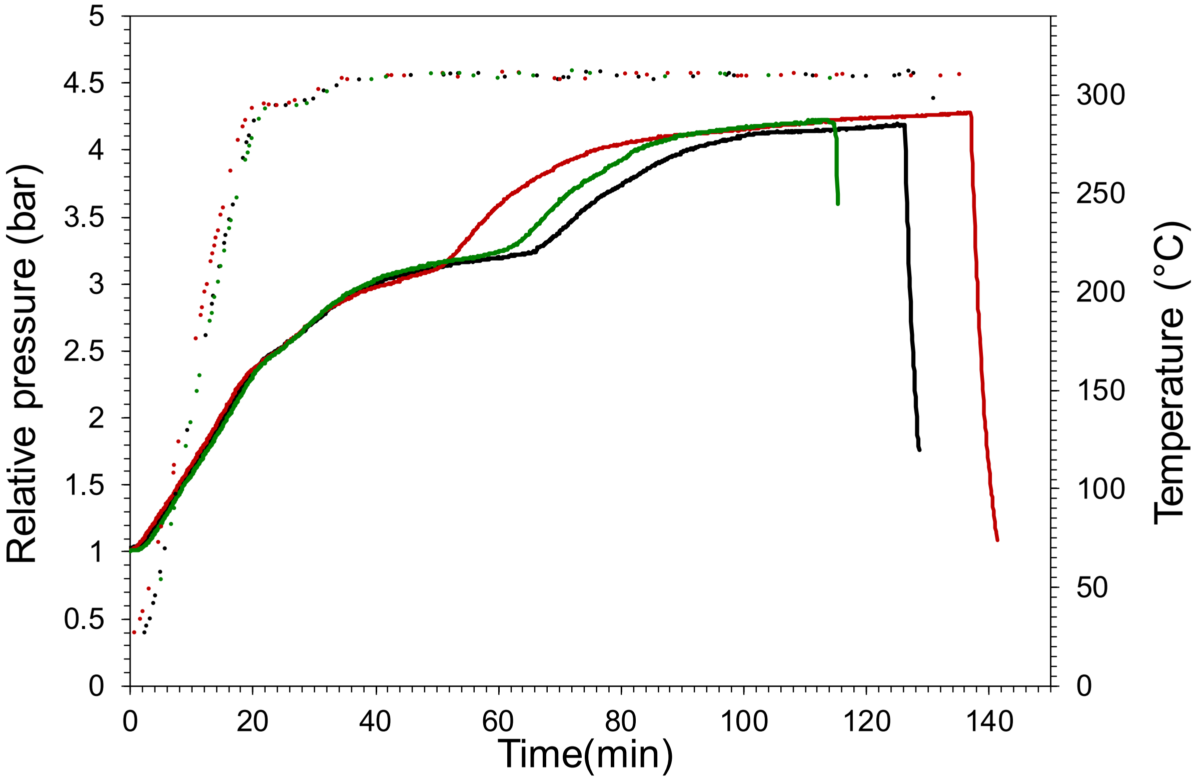

Figure S2. Evolutions of temperature and relative pressure with time of PM-Zn0.30 contact mass during pretreatment at 310 °C for 2 h. The temperature curves are plotted as dashed lines.

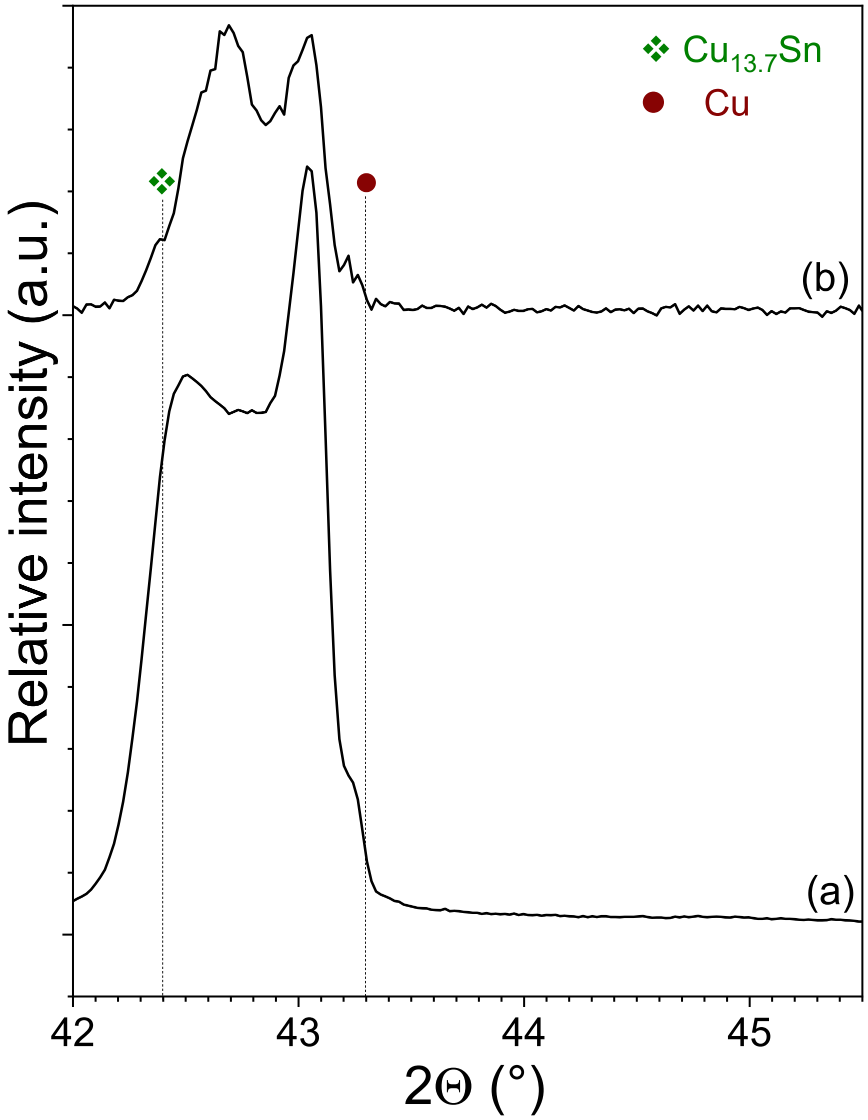

Figure S3. XRD diffractograms in the 2θ angle range of 42-46° of $Cu_{0.9}Sn_{0.1}$ (a) before and (b) after pretreatment at 310 °C. $Cu_{0.9}Sn_{0.1}$ was a mixture of two bronzes. $Cu_{13.7}Sn$ and Cu cubic phases were indexed with the PDF 65-6821 and PDF 04-0836 patterns, respectively.

Table S3. Catalytic performance obtained for three tests with PM-Zn0.30 contact mass pretreated at 310 °C for 30 min.

	$X(CH_3Cl)$ (%)	Si selectivity (%)			
		M2	**M1**	**M3**	**MH**
	90	73	19	3	0.8
	92	76	15	4	1.9
	95	76	15	2	0.9
Average (%)	92	75	16	3	1.2
Standard deviation (%)	2	2	2	1	0.7

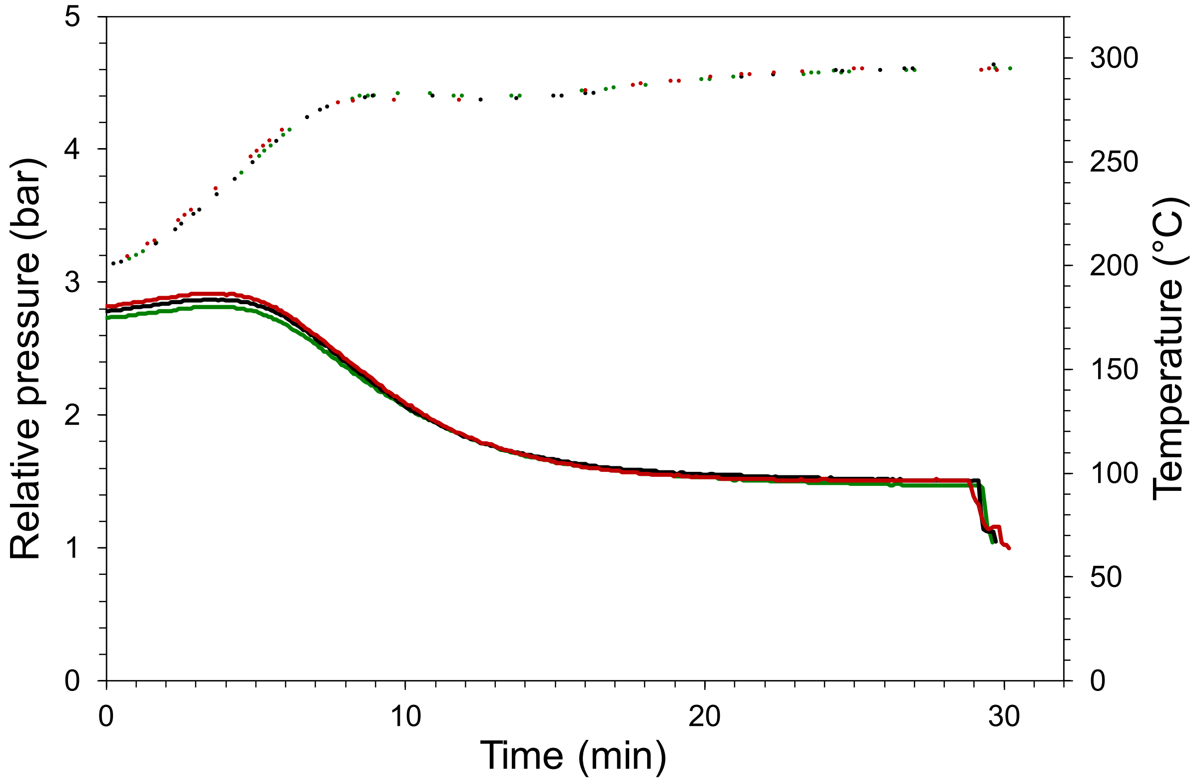

Figure S4. Evolutions of temperature and relative pressure with time of PM-Zn0.30 mass during reaction. The temperature curves rising from 200 to 295 °C are plotted as dashed lines.

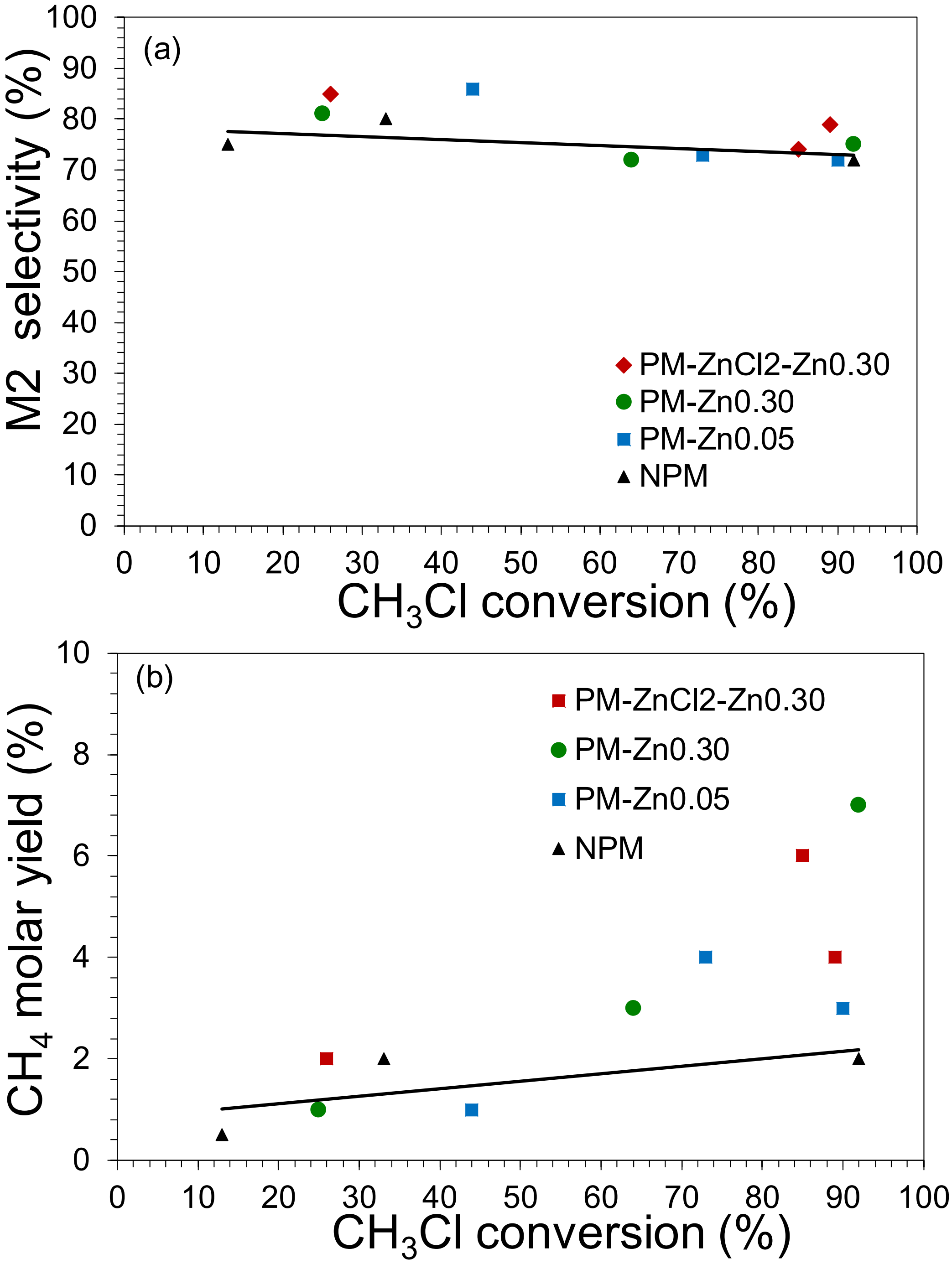

Figure S5. Evolution of the (a) M2 selectivity and (b) CH_4 molar yield with the CH_3Cl conversion at 295 °C for different contact masses.

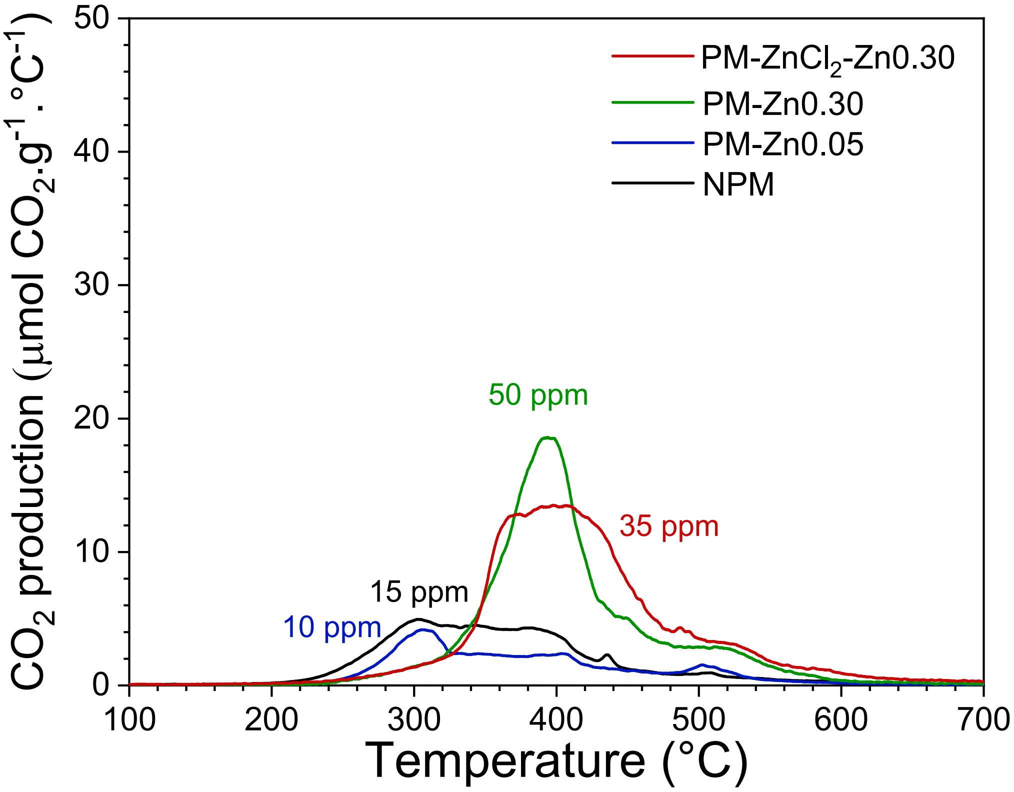

Figure S6. TPO curves of different contact masses after reaction at 295 °C (89-92% of CH_3Cl conversion, 0.5-0.6% of Si conversion).

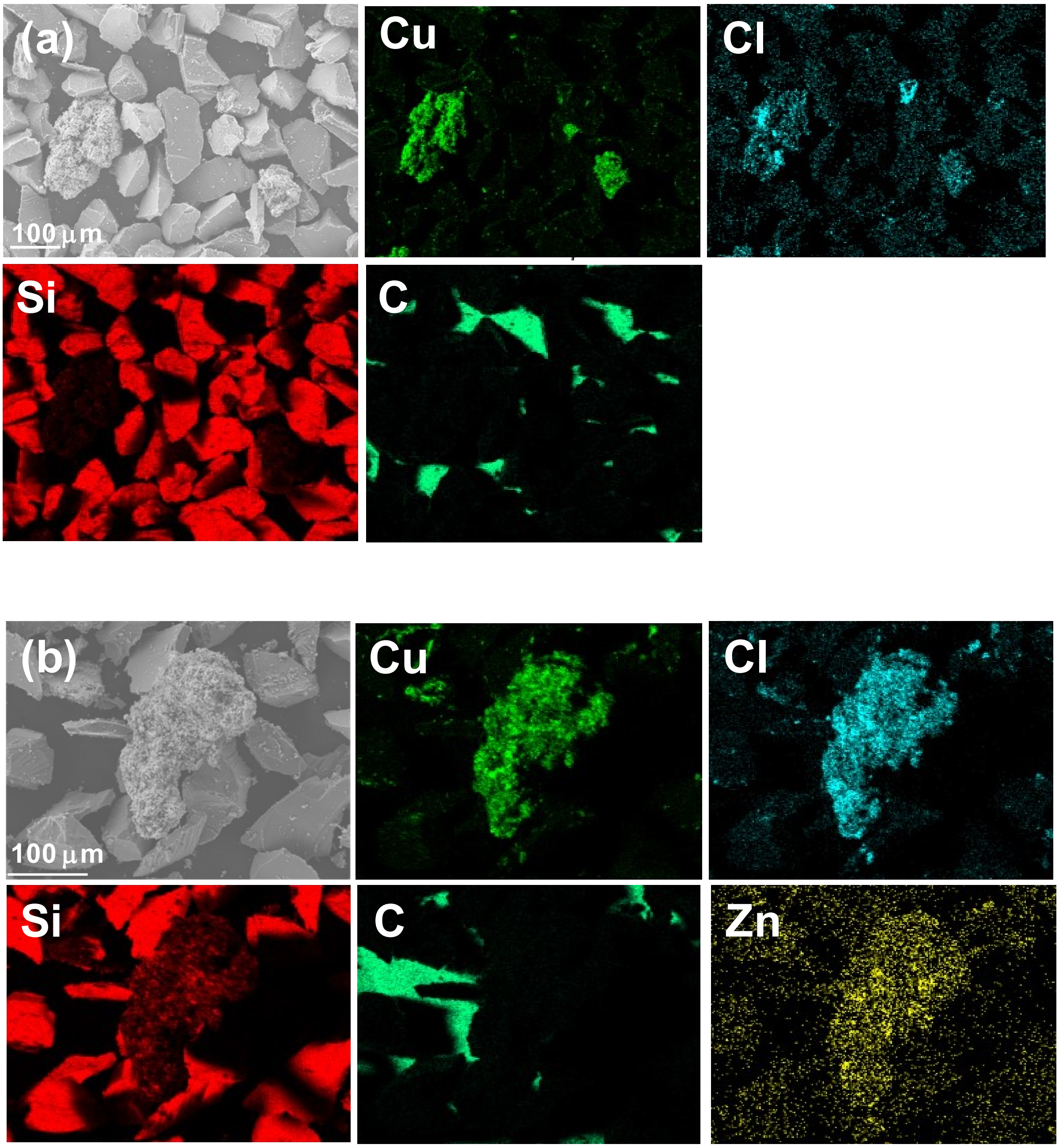

Figure S7. SEM images and corresponding EDS elemental mapping images of the (a) NPM and (b) PM- Zn0.30 contact masses after reaction at 295 °C (89-92% of CH_3Cl conversion, 0.5-0.6% of Si conversion).

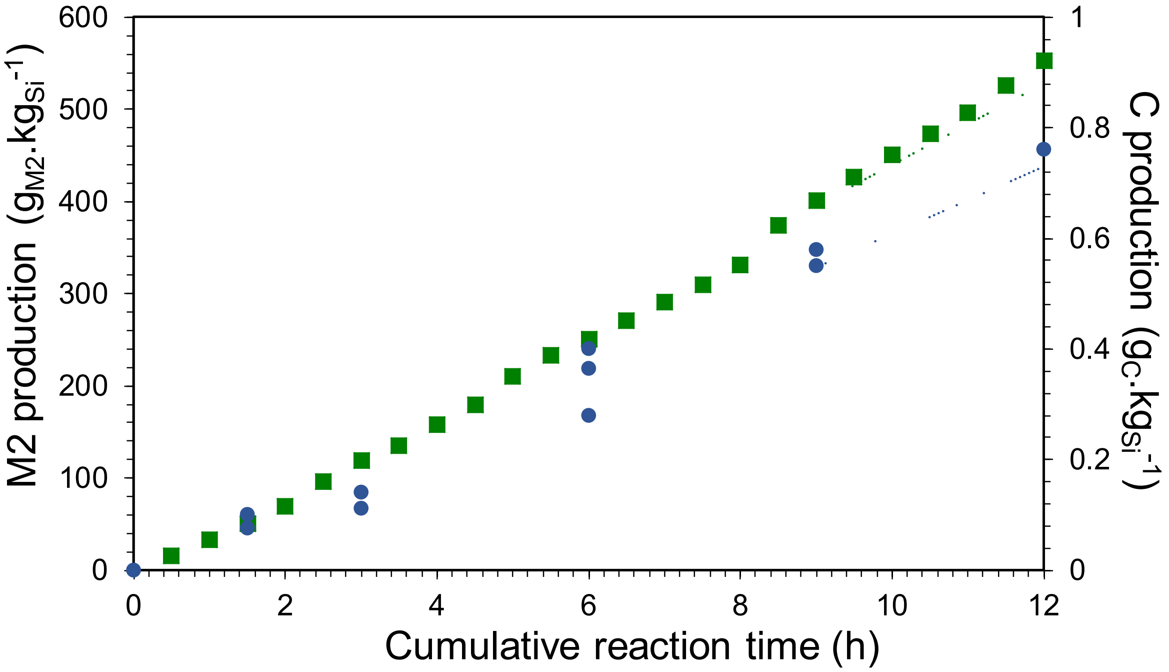

Figure S8. Evolution with cumulative reaction time of C production and M2 production with contact mass PM-Zn0.30 tested after consecutive CH_3Cl injections.

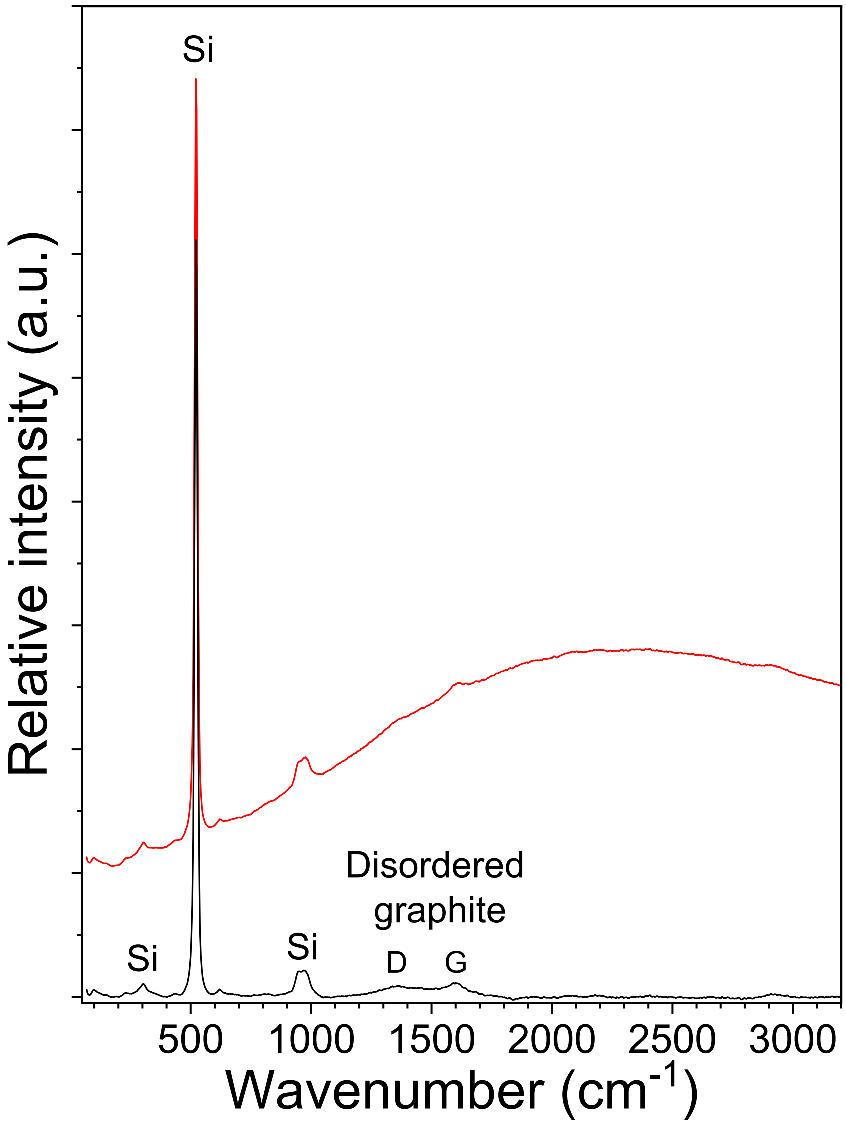

Figure S9. Typical Raman spectrum (a) before and (b) after background subtraction of the PM-Zn0.30 contact mass after reaction at X(Si) = 1.5%.

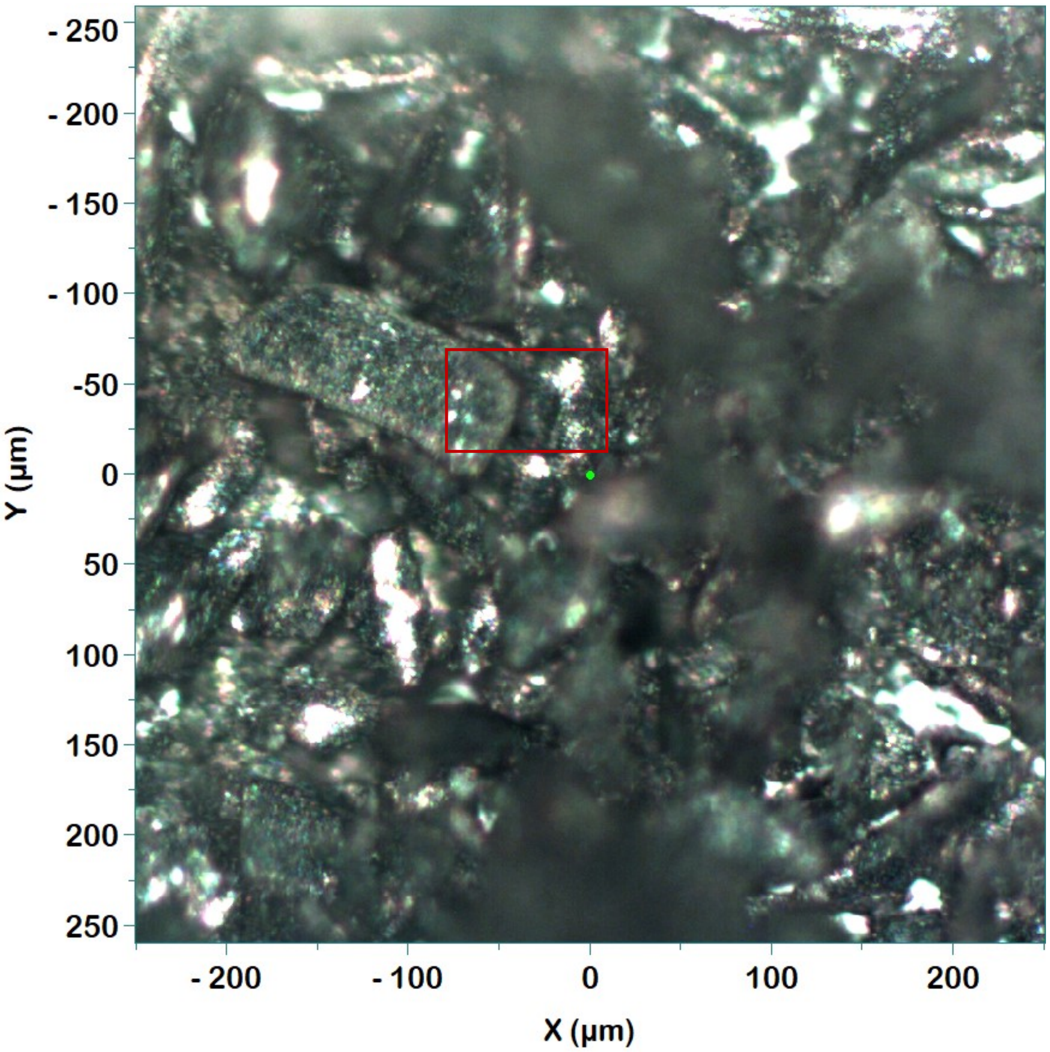

Figure S10. Optical image recorded using a 10x objective of the PM-Zn0.30 contact mass after reaction at X(Si) = 13.9%. The Raman mapping area is outlined in red. The same area was analyzed by SEM and retrieved with Raman spectrometer using a Nano-GPS.

References

1 D. D. Wagman, W. H. Evans, V. B. Parker, R. H. Schumm, I. Halow, S. M. Bailey, K. L. Churney and R. L. Nuttall, *Journal of Physical and Chemical Reference Data*.

2 CRC Handbook of Chemistry and Physics, 84th Edition Edited by David R. Lide (National Institute of Standards and Technology). *J. Am. Chem. Soc.* 2004, **126**, 1586–1586.

3 H. Schimpff, *Zeitschrift für Physikalische Chemie*, 1910, **71U**, 257–300.

4 R. R. Chromik, W. K. Neils and E. J. Cotts, *J. Appl. Phys.*, 1999, **86**, 4273–4281.

5 D. Lüdecke, *Calphad*, 1987, **11**, 135–142.

6 D. Shin, J. E. Saal and Z.-K. Liu, *Calphad*, 2008, **32**, 520–526.